Leibniz Online, Jahrgang 2015, Nr. 20
Zeitschrift der Leibniz-Sozietät e. V.
ISSN 1863-3285
http://www.leibnizsozietaet.de/wp-content/uploads/2015/10/gackstatter.pdf

Fritz Gackstatter

Moon Theory, Tidal Dynamics, and Earthquake Statistics

Bemerkungen zu „Moon Theory, Tidal Dynamics, and Earthquake Statistics“

In der ersten Hälfte der neuen Arbeit werden die für die Erdbebenstudien wichtigen Grundlagen der Mondtheorie entwickelt. Die beiden großen Anomalien Evektion und Variation in der Bewegung des Mondes spielen eine zentrale Rolle.

In Abschnitt 2, Historic Miscellany, berichten wir über die Entdeckungsgeschichte der Anomalien. Johannes Kepler schreibt in seiner *Astronomia Nova*: „Tycho Brahe bemerkte aus Beobachtungen am Mond, die er lange Zeit hindurch sehr häufig bei jeder Stellung zur Sonne ausgeführt hatte, daß beim Mond … die Bewegung … in der Nähe der Konjunktionen und Oppositionen schneller wird.“ Auf Seite 4 der vorliegenden Arbeit findet man den entsprechenden Abschnitt aus Keplers *Astronomia Nova*. Es ist interessant, aus Keplers Fig. 34 (= Figure 1 auf S. 5) Tychos Beobachtung über die schnellere Bewegung in der Nähe der Oppositionen abzulesen.

Hipparchos ist der Entdecker der Evektion. Zu seiner Zeit wurde die lunare Bewegung nur in der Nähe der Voll- und Neumondstellungen beobachtet, die Variationsungleichheit wurde nicht gesehen. Es ist interessant, dass die Evektion einen statistisch signifikanten Einfluss auf die Verteilung der Erdbeben hat; siehe Christoph Gackstatters Beitrag auf den Seiten 800-804 in [11].

In Abschnitt 3 bestimmen wir die Fourierdarstellung der Bahn des Mondes auf der zweiten Näherungsstufe – elliptische Ungleichheit, Evektion und Variation werden berücksichtigt. Wir übersetzen die Parallaxen-Formel in [17, I, S. 161] in eine 1/km-Formel.

In Abschnitt 4 werden die Monate, Jahre und Mondzyklen intensiv studiert, der evektionale Monat U_{eve} und der evektionale Zyklus U_e treten in Erscheinung.

Mit Abschnitt 5 kommen wir zur zweiten Hälfte der neuen Arbeit. Da die Frequenzen der elliptischen Ungleichheit und der Evektion sich wenig unterscheiden entsteht eine Schwebungsinterferenz mit der langen Periode $U_e = 411{,}8$ Tage. Da die Gezeitenkräfte umgekehrt proportional zur dritten Potenz des lunaren Abstandes sind, erwarten wir in den zeitlichen Bereichen mit den hohen Amplituden der Schwebungsoszillationen eine stärkere seismische Aktivität als in den Bereichen mit den kleinen Amplituden. Diese Vermutung wird bestätigt: 1. Siehe Tabelle 5 in Abschnitt 5.5. 2. Siehe das Ergebnis von Christoph Gackstatter über den signifikanten evektionalen Einfluss auf die Verteilung der Erdbeben.

Die drei stärksten Erdbeben im neuen Millennium – Indonesien mit Magnitude 9.1, Chile mit 8.8 und Japan mit 9.0 – fallen in die an die vier extremen Springfluten („maximum“ und „extreme proxigean spring tides“ nach Fergus J. Wood) angrenzenden synodischen Monate. In Abschnitt 5.6 geben wir eine physikalische Erklärung für die starken Beben: extreme Schwankungen in der Torsion des Erdellipsoids sind der Auslöser.

In Abschnitt 7 stellen wir die von Christoph Gackstatter entwickelten statistischen Methoden vor.

Der synodische Monat 2016/10/16 – 2016/11/14 ist die nächste kritische Periode; siehe Tabelle 6. Es besteht die Hoffnung, dass man durch das *„Disaster Alert Mediation using Nature (DAMN)“* Programm der Biologen kritische Regionen eingrenzen kann; siehe Abschnitt 8.2.

Fritz Gackstatter
23. September 2015

Bemerkungen zum starken 2015/09/16 Erdbeben in Chile

Das starke Erdbeben in Chile mit der Magnitude 8.3 ordnet sich in unser System ein:

2015/08/29	F	61' 4.8''			
2015/09/16				8.3	Chile
2015/09/28	F	61' 26.5''	proxigean		
2015/10/27	F	61' 1.3''			

Siehe die ersten beiden Seiten von Woods Tafel 16a in [19]. Wenn wir zusätzlich die „proxigean spring tides“ (siehe Table 4 auf S. 24) heranziehen, dann sehen wir die „proxigean tide“ am 28. September 2015. Zwölf Tage zuvor, am 16. September, wurde das große Beben in Chile ausgelöst.

Adresse des Verfassers:

Prof. Dr. Fritz Gackstatter
Ihnestr. 80
14195 Berlin
e-mail: fgackstatter@gmx.de

Moon Theory, Tidal Dynamics, and Earthquake Statistics

Fritz Gackstatter
Freie Universität Berlin

September 26, 2015

Abstract

In Fergus J. Wood's grand opus on *Tidal Dynamics* [17] lunisolar ephemerides over the period 1600 – 2164 are compiled. In the new millennium four *extreme proxigean spring tides* happened up to now. Surprisingly, the three strongest earthquakes – the 2004 Indonesia Quake with magnitude 9.1, the 2010 Chile Quake with 8.8 and the 2011 Japan Quake with 9.0 – are related to these extreme tides; see [11]. So it is a natural idea to study the lunisolar effect on the trigger of earthquakes.

In Section 3 of the present treatise we develop a second level approximation for the orbit of the Moon which takes the main anomalies evection and variation into consideration. Since the frequencies of elliptic inequality and evection anomaly are only slightly different a beat interference with the long period $U_e = 411.8\,days$ appears. U_e is the evectional cycle. In Section 4 a collection of periods and cycles is presented and period relations are proved. In Figure 5 in Section 5 one can see the beat oscillation of the lunar distance function. We discover a physical argument for the lunisolar influence: In the high amplitude periods of the beat oscillation the seismic activity is above average because tide-raising force varies inversely as the third power of the lunar distance. Finally, in Section 7, we present a result of Christoph Gackstatter developed in [11, p. 800-804]: *The lunar evection anomaly – discovered by Hipparcos and installed in Ptolemy's epicycle theory – has a statistically significant influence on the earthquake distribution.*

The short survey article [19] with the title *Lunisolarer Einfluss auf die Entstehung von Erdbeben* was published recently.

Contents

1 Introduction

In the present treatise we aim to study the lunisolar effect on the trigger of earthquakes. For this reason some basic facts on the moon theory must be compiled. A beat oscillation of the lunar distance function, generated by elliptic inequality and evection anomaly, has an influence on the seismic activity. We are glad that we can use Fergus J. Wood's grand opus on *Tidal Dynamics* [17] together with the *Significant Earthquake Archive* of USGS [18].

1.1 The second level approximation for the orbit of the Moon

In order to find a suitable approximation formula for the lunar orbit we orientate according to Kepler's First Law: *The orbits of the planets are ellipses.* The First Law is a relation on spatial coordinates,

$$\rho = \frac{1}{r} = \frac{1}{p}\{1 + e\ cos\varphi\}, \qquad (I_K)$$

where time t is eliminated; the Second Law takes up time again. $(\rho = \frac{1}{r}, \varphi)$ are polar coordinates with reciprocal radius in the inertial or siderial plane with the Sun in the centre. The separation of space and time is the central idea.

Following the central idea, we look for a law on spatial coordinates describing the lunar orbit. Considering the elliptic inequality as well as the evection

and variation anomaly we find the desired result:

In Euler's synodic plane with the Earth in the centre the following second level approximation for the orbit of the Moon is valid:

$$\rho = \frac{1}{r} = \frac{1}{p}\{1 + e\cos(\frac{U_{syn}}{U_{ano}}\varphi) + f\cos(\frac{U_{syn}}{U_{eve}}\varphi) + g\cos(2\varphi)\}, \qquad (I)$$

where

$$U_{syn} = 29.530\,59\ days, U_{ano} = 27.554\,55\ days, U_{eve} = 31.811\,94\ days \qquad (I_a)$$

are the synodic, anomalistic, and evectional month and

$$e = 0.0545, f = 0.0100, g = 0.0082 \qquad (I_b)$$

the parameters of elliptic inequality as well as evection and variation anomaly. $p = 384,397\ km$ *is the mean lunar distance.*

$(\rho = \frac{1}{r}, \varphi)$ are polar coordinates in Euler's rotating or synodic plane with the Earth in the centre. In Table 2 in Section 4.1 one can find a collection of periods and their numerical values. Because of $e, f, g > 0$ in (I) the lunar distance is minimal in the direction $\varphi = 0$ of the full moon. Since perigee and full moon do not coincide in real nature a problem arises. Fortunately we can handle the problem with Fergus J. Wood's tidal tables where we can find dates with small perigee-syzygy separation. For example, on January 4, 1912, the difference between full moon and perigee only amounts to six time minutes. In Section 3 we will develop formula (I) and discuss the initial date problem.

If we neglect the big anomalies evection and variation ($f = g = 0$ in (I)) the first approximation level remains, if we aim at a higher level, further Fourier terms must be worked into (I).

From the second level approximation (I) we can read a beat oscillation of the lunar distance function which has an effect on the trigger of earthquakes. These facts will be studied in Section 5.

1.2 The lunisolar effect on the trigger of earthquakes

When the Moon is full or new, the gravitational pull of the Moon and Sun are combined and spring tides are the consequence. High spring tides occur when the Moon is close to the Earth on its elliptical path because tide-raising force varies inversely as the third power of the lunar distance. A beat oscillation of the lunar distance function, generated by elliptic inequlity and evection anomaly in (I), result in corresponding swaying of the tide-raising forces. So one can expect that in the high amplitude periods of the beat oscillation the seismic activity is above average. This conjecture is proved true:

1. In the new millennium four *extreme proxigean spring tides* happened up to now, and the big 8.8+ earthquakes occured in adjoining synodic months:

the 2004 Indonesia Quake with magnitude 9.1, the 2010 Chile Quake with 8.8, and the 2011 Japan Quake with 9.0. In Section 5 we present Fergus Wood's definition of an *extreme proxigean tide*.

2. In 2010 Christoph Gackstatter made a complete statistical test for the entirety of measured quakes. More than 650,000 earthquakes and 13,860 observations, which is the total number of days in the database, are used for the linear regression; see [11, p. 800-804]. With the small 1.83% p-value a fundamental result is proved: **The lunar evection anomaly, discovered by Hipparcos and installed in Ptolemy's epicycle theory, has a statistically significant influence on the earthquake distribution.**

Influences the Moon the creation of earthquakes? This question was discussed controversial in the past. Now we have the statistically significant result that the evectional beat oscillation of the lunar distance function has an influence on the earthquake distribution. In our computer epoch statistics can handle huge observation data. In Section 7 we present further details.

2 Historic miscellany

Hipparcos ($\sim$ 180 – 125 BC), one of the greatest astronomers of the classic antiquity, is the discoverer of the evection anomaly. Because of $U_{syn} = 29.5\,days$ and $U_{eve} = 31.8\,days$ the evectional disturbance of the mean longitudinal motion sometimes appears close by the syzygys, sometimes it is not much in evidence there. This inequality in the motion of the Moon was detected by Hipparcos. **Ptolemy** ($\sim 90 - 160$) pays attention to the anomaly when creating his epicycle theory. For further details see K. Stumpff's grand opus on Celestial Mechanics [15, I, p. 34].

In 1590 **Tycho Brahe** discovered the variation anomaly. Because of the variation period $\frac{1}{2}U_{syn}$ no inequality in the motion of the Moon can be seen in syzygy directions. Paying attention to all lunar positions relative to the Sun the grand observer Tycho detected the anomaly: the motion becomes quicker close by the oppositions and conjunctions and slower at the quadrature points. This new oscillation, now designated as variation anomaly, stands on a level with elliptic inequality and evection anomaly. **Johannes Kepler** reports on Tycho's discovery in his opus *Astronomia Nova* [1, AN, p. 252]:

Animadvertit TYCHO BRAHEVS per diutinas et creberrimas observationes Lunae in omni situ cum Sole, quod in Luna praeter anomaliam epicycli, et praeter illam anomaliam menstruam, quae etiam PTOLEMAEO nota fuit, ipse etiam medius motus nondum sit plane medius, sed intendatur sub conjunctiones et oppositiones cum Sole, remittatur in quadraturis.

There is a German translation of the *Astronomia Nova* by M. Caspar and an English translation by W.H. Donahue; see entry [1] in the References.

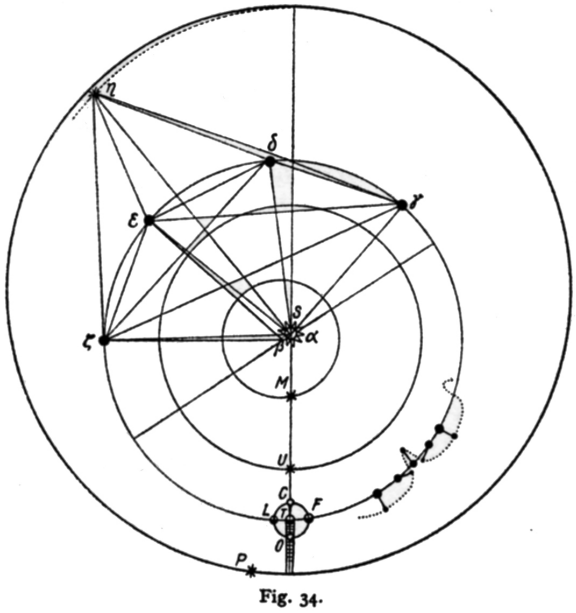

Figure 1: Kepler's graph of Tycho's observation

In Fig. 34 in [1, AN] Kepler presents a graph of the lunar orbit where the variation anomaly can be recognized. We adopt Kepler's graph in Figure 1.

In Figure 1 we see a small circle with opposition point O, conjunktion point C, and the quadrature points L and F. This circle is the orbit of the Moon in a synodic sense and can be compared with the lunar orbit in the synodic box in Figure 3 in Section 3.2. The punctured curve is the orbit of the Moon in the inertial or sidereal plane. Painting five Earth-Moon constellations Kepler shows the quick motion of the Moon at the oppositions.

The meeting of Tycho and Kepler in Benatek and Prague was a good coincidence for natural science. *Max Brod* describes their living together in his novel *Tycho Brahes Weg zu Gott* published by Wolff Verlag in Leipzig in 1915. Entry [1] in the References contains further data on Kepler's work.

A further landmark in the development of the moon theory is due to **Isaac Newton**. On April 21, 1686, Halley informed the Royal Society that Newton's work with the title *Philosophiae Naturalis Principia Mathematica* would be ready for print. This first edition contains a proposal for solving the 3-body problem. Furthermore, the different anomalies in the motion of the Moon are handled in a unified manner. But Newton had a problem with the apsides period, so he later reveals to his colleague John Machin that his head never ached but with his study on the Moon. Richard Westfall's biography [2] is recommendable. A wonderful representation of the history of astronomy up to Newton we

find in A. Koestler's book on the sleepwalkers [3].

The Universal Law of Gravitation is one of Newton's great discoveries. All of Kepler's Laws follow as a direct consequence of the Universal Law. Newton created the foundation for the research of Leonhard Euler, G.W. Hill, and E.W. Brown mentioned next.

We have to include **Leonhard Euler** in our list. In [4] we quote Euler's two moon theories: *Theoria motus lunae* (Berlin 1753) and *Theoria motuum lunae* (Saint Petersburg 1772). Euler introduced the rotating or synodic system of coordinates in his second book.

Euler's first theory had an important practical application: After a shipping disaster the British Board of Longitude opened a price competition with the aim to improve the navigation possibilities on the high seas. Using Euler's moon theory **Tobias Mayer** developed a method and submitted it to the Board in 1755. Mayer's widow, Euler and the constructor of a chronometer, **John Harisson**, shared the prize.

In the lecture *Eulers Beiträge zu Variationsrechnung und Himmelsmechanik* [9, Sitzungsber. Leibniz-Soz. Berlin, Band 94, p. 57-65, 2008] and in the supplementation of Dieter B. Herrmann on page 66 one can find further information on Euler's and Mayer's work.

Finally, we mention **G.W. Hill** and **E.W. Brown**. The methods of the restricted 3-body analysis are the basis of G.W. Hill's famous moon theory. Earth and Sun are the primaries and the Moon orbits around the Earth in Euler's rotating or synodic system of coordinates. By using proper simplifications Hill developed the potential

$$\Omega = \frac{3}{2}x^2 + \frac{1}{r} \tag{1}$$

which enters into Newton's equation of motion for the Moon:

$$\ddot{x} - 2\dot{y} = \frac{\partial \Omega}{\partial x},\ \ddot{y} + 2\dot{x} = \frac{\partial \Omega}{\partial y}. \tag{2}$$

Hill's variation orbit, sketched in Figure 2, is an important solution of system (2); we adopt on the whole Stumpff's picture in [15, II, p. 519].

The variation orbit is related to the variation anomaly of the Moon. In Figure 2 we see that the central distance of the test body on Hill's orbit becomes smaller close by the oppositions and conjunctions and bigger at the quadrature points. Smaller distance – quicker motion, bigger distance – slower motion: Tycho's observation and Hill's orbit go well together.

We recommend two references: Karl Stumpff's opus on celestial mechanics [15, II, p. 56-60 and p. 511-522] and Victor Szebehely's *Theory of Orbits* [16, p. 602-629]. Szebehely's book can be regarded as the encyclopaedia of the restricted 3-body analysis.

Hill published his famous moon theory in [5]. It is the basis of the research of E.W. Brown who is the creator of the most accurate theory on the lunar motion.

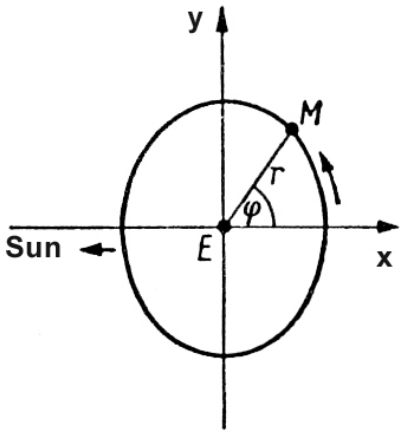

Figure 2: Variation orbit of the moon theory in the synodic plane

With the advent of digital computers Brown's Fourier expansions, given to his 1919 tables, began to be used for computation.

In Fergus Wood's *Tidal Dynamics* we recognize the importance of Brown's *Improved Lunar Ephemeris*. In Tables 16 and 16a in [17, I, p. 159-218] lunisolar ephemerides are presented over the period 1600 – 2164 with great exactness. At the beginning of the Tables, on pages 160 to 165, we see long Fourier expansions for the elements of motion of the Moon. Wood's Tables will play an important part in the subsequent earthquake research.

3 The second level approximation for the orbit of the Moon

3.1 The big anomalies

Of course, on the first approximation level Kepler's Laws determine the motion of the Earth's satellite. However, the influence of the disturbing attraction of the Sun is tremendous, so the rules of the 3-body analysis must be taken into account on the next approximation step. It is not surprising that anomalous librations disturb the lunar motion.

The **variation anomaly** must be mentioned first; its period $\frac{1}{2}U_{syn}$ with the synodic month

$$U_{syn} = 29.530\,59\,days \tag{3}$$

shows the direct influence of the Sun. The synodic period is the time interval from new moon to new moon. The single periods have different lengths. In Fergus Wood's *Tidal Dynamics* one can find fluctuation data in Table 17 in [17, I, p. 231-239], a difference of $0.54\,days$ in the length of the synodic periods is

possible. In (3) we see the mean value U_{syn} of the periods U measured over a long time of observation.

The 3-body system Sun-Earth-Moon cannot endure **elliptic inequality** and variation alone, so a motion of compensation, the **evection anomaly**, is necessary. When developing the Fourier expansions for the lunar orbit the evection comes into play via the addition formulas of the trigonometric functions.

In the expansion of the ecliptic longitude of the Moon one can see the power of the anomalies:

$$\begin{aligned} \text{true longitude} = \text{mean longitude} & \\ + 377.3' \sin L + \ldots & \quad \text{(elliptic inequality)} \\ + 76.4' \sin(2D - L) + \ldots & \quad \text{(evection)} \\ + 39.5' \sin(2D) + \ldots & \quad \text{(variation)} \\ + \ldots & \end{aligned} \tag{II}$$

The numerical values are taken from Karl Stumpff's work on celestial mechanics [15, I, p. 38]. Surprisingly, the motion of compensation is stronger than the variation trigger.

Two further main anomalies are the **revolution of the line of apsides** and the **revolution of the nodes**. In Section 4.6 the simple approximation formula (51) on the period of nodes is developed. For this reason we can withdraw into the synodic plane and deal only with variation, evection and apsides revolution in the future.

3.2 Euler's synodic system of coordinates and Hill's time normalization

Have a look at the three celestial bodies Sun, Earth and Moon in Figure 3. Out of the box we see the inertial or **sidereal plane**. The Sun is in the centre of the plane, the Earth circles around the Sun with angular velocity n and the Moon orbits around the Earth. To study the complicated course of the Moon it is advantageous to work in the rotating or **synodic plane**. The straight line through Sun and Earth is the abscissa of the synodic system, the perpendicular line through the Earth is the ordinate. Of course, the planet is in the centre of the plane in the moon theory. In the box we see the synodic system and the orbit of the Moon relative to the new x- and y-axis. In 1772 Euler introduced the rotating system of coordinates; it is the basis of his second moon theory in [4].

In Hill's moon theory we have the normalization $n = 1$ for the angular velocity of the Earth. Evidently, the transformation formula is

$$t[Hill's\ time] : 2\pi = \tau[days] : U_s \tag{4}$$

with the sidereal year

$$U_s = 365.256\,36\ days. \tag{5}$$

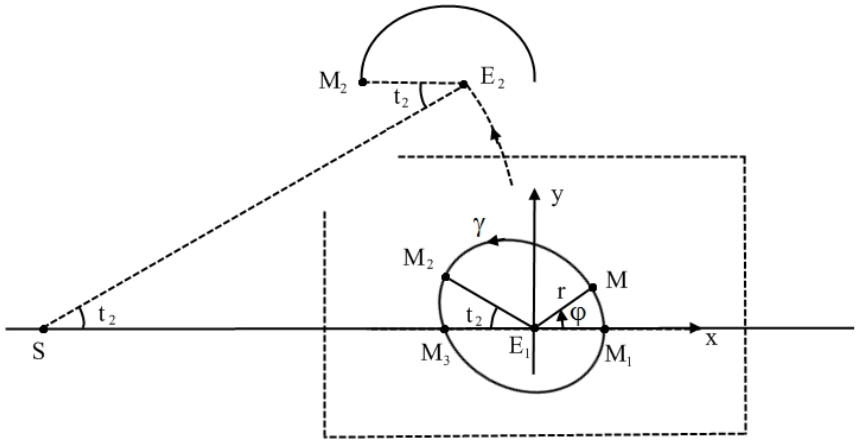

Figure 3: The orbit of the Moon in the sidereal system and in the synodic system in the box

Example: For its way from M_1 to M_3 in Figure 3 the Moon needs the period $\frac{1}{2}U_{syn}$. Starting with $t_1 = 0$ we find

$$t_3 = \frac{U_{syn}}{U_s}\pi \tag{6}$$

on Hill's scale.

Finally we determine the mean longitude φ_m in formula (II) by decoding Figure 3. The mean longitude is linear in t; without restriction we start with $\varphi_m(t_1) = 0$ for $t_1 = 0$ and set $\varphi_m = Pt$.

Proposition: The mean longitude part in (II) relative to Hill's time t is

$$\varphi_m = \frac{U_s}{U_{syn}}t = \frac{365.256\,36}{29.530\,59}t = 12.368\,74\,t. \tag{7}$$

Proof: In the course of half a synodic month the angle φ_m in the synodic box in Figure 3 increases from $\varphi_m(t_1) = 0$ up to $\varphi_m(t_3) = \pi$. Hill's time t_3 is calculated in (6), and inserting it into (7) we find the desired result:

$$\varphi_m(t_3) = \frac{U_s}{U_{syn}}t_3 = \frac{U_s}{U_{syn}}\frac{U_{syn}}{U_s}\pi = \pi. \tag{8}$$

Since the linear relation (7) is checked for t_3, it is valid for all t, q.e.d. The corresponding quantity to U_s/U_{syn} in Stumpff's investigation is $\nu = \nu' - 1$; see [15, II, p. 520].

3.3 E.W. Brown, F.J. Wood and the coefficients of the Fourier expansion

The basic formula for our program we find in Fergus Wood's *Tidal Dynamics*. In Tables 16 and 16a in [17, I, p. 159-218] lunisolar ephemerides are presented over the period 1600 – 2164. To determine these precise data the long Fourier expansions on pages 160 to 165 are used. We recognize the importance of E.W. Browns *Improved Lunar Ephemeris*. Let us start with the expansion for parallax π on page 161:

$$\begin{aligned} \pi = {} & 3422.608 && \text{(mean parallax)} \\ & + 186.540\cos L + \ldots && \text{(elliptic inequality)} \\ & + 34.312\cos(2D - L) + \ldots && \text{(evection)} \\ & + 28.233\cos(2D) + \ldots && \text{(variation)} \\ & + \ldots \end{aligned} \tag{9}$$

The lunar parallax as a measure of distance is defined as the apparent equatorial angular semi-diameter of the Earth as it would be seen from a position at the centre of the Moon. We take over the evection argument $2D - L$ used in (II). The Fourier coefficients are related to arc seconds. For our second level approximation we only have to list the big terms in (9). In the first line the mean parallax of the Moon,

$$\pi_m = 3422.608'' = 57'\,2.608'' = 0.954\,724^\circ, \tag{10}$$

is registered and the mean km value of the lunar distance is

$$p = \frac{6378.14}{sin\pi_m} = 384\,397\ km; \tag{11}$$

see [17, I, p. 22, 27].

Kepler's First Law (I_K) steers the following calculations. It is

$$\pi = \pi_m\{1 + e\cos L + f\cos(2D - L) + g\cos(2D) + \ldots\} \tag{12}$$

with

$$e = \frac{186.540}{3422.608} = 0.054\,502,\ f = 0.010\,025,\ g = 0.008\,249. \tag{13}$$

Now we translate the parallax formula (9) into a $1/km$ formula:

$$\frac{\sin\pi}{6378.14} = \frac{\sin[\pi_m\{1 + e\cos L + f\cos(2D - L) + g\cos(2D) + \ldots\}]}{6378.14}. \tag{14}$$

On the left-hand side the reciprocal radius of the Moon appears:

$$\frac{sin\pi}{6378.14} = \frac{1}{r} = \rho. \tag{15}$$

A good approximation for the right-hand side is

$$\frac{\sin \pi_m}{6378.14} \times \{1 + e \cos L + f \cos(2D - L) + g \cos(2D) + \dots\} \tag{16}$$

with the reciprocal of the mean distance $1/p$ as prefactor.

Test of the quality of the approximation on the right-hand side: On 1912/01/04 a full moon with maximal parallax $\pi_{max} = 61' 31.6''$ appeared. According to Wood's tables it is the biggest parallax in the period 1600 – 2164. Inserting into formula (12) yields

$$\pi_{max} = 3691.6'' = 3422.608''\{1 + 0.078\,592\,7\} = \pi_m\{1 + 0.078\,592\,7\}. \tag{17}$$

We have to compare the values of (14) and (16): It is

$$\frac{\sin[\pi_m\{1 + 0.078\,592\,7\}]}{6378.14} = \frac{\sin \pi_{max}}{6378.14} = 2.805\,912 \cdot 10^{-6}, \tag{18}$$

and the reciprocal value $r_{min} = 356\,390\ km$ is the distance of the Moon on 1912/01/04. For the approximation (16) we find

$$\frac{\sin \pi_m}{6378.14} \times \{1 + 0.078\,592\,7\} = 2.805\,937 \cdot 10^{-6} \tag{19}$$

and $r = 356\,387\ km$. The approximate distance is $\sim 3\ km$ smaller than r_{min}. On the other side, the approximate value is $\sim 3\ km$ bigger than r_{max}. For the other r-values the km difference is even smaller. If essential we can compensate the difference.

To sum it up, the $1/km$ relation

$$\rho = \frac{1}{r} = \frac{1}{p}\{1 + e \cos L + f \cos(2D - L) + g \cos(2D) + \dots\} \tag{20}$$

is a good approximation of the parallax formula (9). The Fourier expansion for parallax π in [17, I, p. 161] holds 37 terms. We can put in all these terms in our km formula, too.

The next problem is the study of the arguments of the cos functions.

3.4 The arguments of the Fourier expansion

The variation term $g \cos(2D)$ in (20) is assigned to the variation orbit of the Moon in the synodic plane in Figure 2, so $g \cos(2\varphi)$ is the substitute in the (ρ, φ) coordinate system and

$$D = \varphi. \tag{21}$$

The period is $\frac{1}{2}U_{syn}$ and, because of $g = 0.008\,249 > 0$, the distance of the Moon becomes smaller close by the oppositions and conjunctions and bigger at

the quadrature points. We pay attention to Tycho's observation.

Finally, we determine the arguments of elliptic inequality and evection anomaly. As sketched in Figure 3 we assume that M_1 is a perigee position for the Moon with $t_1 = 0$ and $\varphi(t_1) = 0$. We have to set $L(t_1) = 0$, $(2D - L)(t_1) = 0$ and $2D(t_1) = 0$, then

$$\frac{1}{r(t_1)} = \frac{1}{p}\{1 + e + f + g + \dots\} \tag{22}$$

and, because of $e, f, g > 0$, the perigee precondition is taken into account.

The elliptic term $e \cos L$ arranges the apsides revolution, so the **anomalistic month**

$$U_{ano} = 27.554\,55\, days \tag{23}$$

must be introduced. The anomalistic period is the time interval from perigee to perigee. The single periods have different lengths because of the influence of evection, variation, and other anomalies. In (23) we see the mean value U_{ano} of the periods U measured over a long time of observation. Table 17 in [17, I, p. 231-239], already mentioned in Section 3.1, also contains fluctuation data on anomalistic periods.

For the argument L of the elliptic term we need a linear relation which only contains mean values. Proposition: Related to Hill's time t it is

$$L = \frac{U_s}{U_{ano}} t. \tag{24}$$

$L(t_1) = 0$ for $t_1 = 0$ is taken into consideration.

Proof: In Figure 3 we see the perigee M_1 and the next apogee M_2. For its way from M_1 to M_2 the Moon needs the period $\frac{1}{2} U_{ano}$. Starting with $t_1 = 0$ translation formula (4) yields

$$t_2 = \frac{U_{ano}}{U_s} \pi \tag{25}$$

on Hill's scale. The argument L increases from $L(t_1) = 0$ up to $L(t_2) = \pi$. Inserting t_2 into (24) we find the desired result:

$$L(t_2) = \frac{U_s}{U_{ano}} \frac{U_{ano}}{U_s} \pi = \pi. \tag{26}$$

Since the linear relation (24) is checked for t_2, it is valid for all t, q.e.d.

The term $f \cos(2D - L)$ takes care of the evection anomaly in (20), so the **evectional month**

$$U_{eve} = 31.811\,94\, days \tag{27}$$

must be introduced. The evectional month is not so common as the months mentioned so far, a derivation of the numerical value will be supplemented in

Section 3.5. The evectional period is the time interval between the parallax maxima of the evectional deviation – in other words: the time interval from "evectional perigee" to "evectional perigee". Of course, the single periods have different lengths and sway around the mean value U_{eve}.

For the argument $2D-L$ we need a linear relation which only contains mean values. Proposition: Related to Hill's time t it is

$$2D - L = \frac{U_s}{U_{eve}} t. \tag{28}$$

$(2D - L)(t_1) = 0$ for $t_1 = 0$ is taken into consideration.

Proof: Approximately *one* day after having passed M_3 in Figure 3 the Moon comes to the "evectional apogee" M_4. For its way from M_1 to M_4 the period $\frac{1}{2}\, U_{eve}$ is needed. Starting with $t_1 = 0$ translation formula (4) yields

$$t_4 = \frac{U_{eve}}{U_s} \pi \tag{29}$$

on Hill's scale. The argument $2D - L$ increases from $(2D - L)(t_1) = 0$ up to $(2D - L)(t_4) = \pi$. Inserting t_4 into (28) we find the desired result:

$$(2D - L)(t_4) = \frac{U_s}{U_{eve}} \frac{U_{eve}}{U_s} \pi = \pi. \tag{30}$$

Since the linear relation (28) is checked for t_4, it is valied for all t, q.e.d.

With (II) and (7) we find the passage from Hill's time t to longitude φ:

$$\varphi = \varphi_m + \cdots = \frac{U_s}{U_{syn}} t + \ldots \;\; and \;\; t = \frac{U_{syn}}{U_s} \varphi + \ldots \,. \tag{31}$$

Replacing t in (24) and (28) by the mean value term in (31) we arrive at the φ formulas

$$L = \frac{U_{syn}}{U_{ano}} \varphi \;\; and \;\; 2D - L = \frac{U_{syn}}{U_{eve}} \varphi \tag{32}$$

for the arguments.

Interim result: As sketched in Figure 3 we assume that M_1 is a perigee position for the Moon. In this case we developed the (r, φ) formula

$$\rho = \frac{1}{r} = \frac{1}{p} \{1 + e \cos(\frac{U_{syn}}{U_{ano}} \varphi) + f \cos(\frac{U_{syn}}{U_{eve}} \varphi) + g \cos(2\varphi) + \ldots \} \tag{33}$$

for the lunar orbit.

3.5 The evectional month and the Harmonic Theorem

Comparing the arguments in (20) and (33) yields

$$\frac{U_{syn}}{U_{eve}} \varphi = 2D - L = 2\varphi - \frac{U_{syn}}{U_{ano}} \varphi, \;\; \frac{1}{U_{eve}} = \frac{2}{U_{syn}} - \frac{1}{U_{ano}} \tag{34}$$

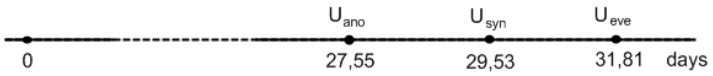

Figure 4: The harmonic periods

and the numerical value of U_{eve} amounts to

$$U_{eve} = \frac{U_{syn}U_{ano}}{2U_{ano} - U_{syn}} = 31.811\,94\ days. \tag{35}$$

3.5.1 Kepler's Harmonice Mundi

Finally we point to a property in Kepler's spirit.

Harmonic Theorem: *The synodic month is the harmonic mean of anomalistic and evectional month,*

$$\frac{1}{2}(\frac{1}{U_{ano}} + \frac{1}{U_{eve}}) = \frac{1}{U_{syn}}. \tag{36}$$

In the motion of the three celestial bodies Sun, Earth and Moon there are striking constellations and periods: the new and full moon positions and the month U_{syn}, perigee and apogee with U_{ano}, the variation with $\frac{1}{2}U_{syn}$, and the evectional compensation with U_{eve}. Formula (36) connects these periods in a harmonic way. U_{sid} does not appear because the three bodies do not pay attention to the sidereal system. In Figure 4 one can see the proportion of the three months.

My endeavour to find the *Harmonic Theorem* in the literature led me to Kepler's opus *Harmonices Mundi Libri V* [1, HM]. In Chapter III of Liber III, which is devoted to music, the *Harmonic Proportion* is discussed:

If a and b are given numbers with $a < b$, then $\frac{2ab}{a+b}$ is the harmonic mean of a and b and the quotient $a : \frac{2ab}{a+b} = \frac{a+b}{2} : b$ is termed *Harmonic Proportion.*

The periods U_{ano}, U_{syn} and U_{eve} mark three points on the line in Figure 4 which lie in a harmonic position, so the Harmonic Proportion can be assigned:

$$U_{ano} : U_{syn} = 27.554\,55 : 29.530\,59 = 0.933\,085 \approx 14 : 15 = 0.933\,333. \tag{37}$$

14/15 is a "small-integer approximation" of the Harmonic Proportion.

Surprisingly, the fraction 14/15 appears again in another connection in *Harmonice Mundi.* In Chapter IX of Liber V, which is devoted to astronomy, Kepler assigns proportion values to the motion of the planets; Proposition XXVIII says

in original Latin:

Telluri propria motuum proportio competebat 14.15. circiter: Veneri 35.36. circiter.

The proportion 14/15 belongs to the motion of the Earth and according to Kepler's proof it is a "small-integer approximation" to

$$2916 : 3125 = 0.933\,120; \tag{38}$$

so the difference between the exact values in (37) and (38) is smaller than $4 \cdot 10^{-5}$.

The proportion 14/15 appears both in the revolution of the Moon around the Earth and in the revolution of the Earth around the Sun, so we can deduce the

Musical Theorem: *The motions of Earth and Moon play the same sound in the music of spheres of the solar system.*

One can speculate that the Moon has taken over the harmony when splitting off from the Earth. After this excursion into Kepler's world of ideas we descend to our approximation program.

3.6 Perigee-syzygy separation and the second level approximation for the orbit of the Moon

Let us assume that $e > 0$ in (I_K) . Then the perihelion lies in the direction $\varphi = 0$. This initial condition can be fulfilled in every sidereal year of the planet.

Because of $e, f, g > 0$ in (13) and (33) the perigee lies in the full moon direction $\varphi = 0$. Since one cannot expect that perigee and full moon coincide in real nature a problem arises. Fortunately, we can handle the problem with the aid of Fergus Wood's *Tidal Dynamics*. In column 9 of Tables 16 and 16a in [17, I] one can find full moon dates with small perigee-syzygy separation $|P - S|$. Nine present-time examples are:

2007/10/26	F	P-S = 7 hours	$\pi = 61'26.9''$
2008/12/12	F	P-S = 5 hours	$\pi = 61'29.3''$
2010/01/30	F	P-S = 3 hours	$\pi = 61'29.3''$
2011/03/19	F	P-S = 1 hour	$\pi = 61'29.6''$
2012/05/06	F	P-S = -1 hour	$\pi = 61'25.7''$
2013/06/23	F	P-S = -1 hour	$\pi = 61'25.3''$
2014/08/10	F	P-S = 0 hours	$\pi = 61'26.3''$
2015/09/28	F	P-S = -1 hour	$\pi = 61'26.5''$
2016/11/14	F	P-S = -2 hours	$\pi = 61'30.2''$

Table 1. Dates with small perigee-syzygy separation

We see the development of the perigee-syzygy separation in $14 \times U_{syn}$ steps and the development of the lunar parallax. In 2014/08/10 the time difference between perigee and full moon is less than half an hour. This date is a good initial value for our Fourier expansion.

Approximation formula for the orbit of the Moon: *Let us introduce polar coordinates with reciprocal radius* $(\rho = \frac{1}{r}, \varphi)$ *in Euler's rotating or synodic plane with the Earth in the centre. We assume that* $\varphi_1 = 0$ *is related to* 2014/08/10. *Then the following second level approximation formula is valid:*

$$\rho = \frac{1}{r} = \frac{1}{p}\{1 + e\cos(\frac{U_{syn}}{U_{ano}}\varphi) + f\cos(\frac{U_{syn}}{U_{eve}}\varphi) + g\cos(2\varphi)\}, \qquad (I)$$

where

$$U_{syn} = 29.530\,59\ days,\ U_{ano} = 27.554\,55\ days,\ U_{eve} = 31.811\,94\ days \qquad (I_a)$$

are the synodic, anomalistic, and evectional month and

$$e = 0.054\,502,\ f = 0.010\,025,\ g = 0.008\,249 \qquad (I_b)$$

the parameters of elliptic inequality as well as evection and variation anomaly. $p = 384\,397\ km$ *is the mean lunar distance.*

Remarks: 1. Formula (I) takes into consideration the big anomalies evection, variation and the revolution of the line of apsides. The e term steers the apsides revolution. One can improve the quality of the approximation by adding further terms of the Fourier expansion for parallax π in [17, I, p. 161].

2. Kepler's Second Law, the area theorem, connects angular φ and time t. An elementary integral of arctan type describes the function $t = t(\varphi)$ for the planetary orbits. In the lunar case the mean longitude formula (7) makes a passage from φ to t possible – on a low approximation level. In [17, I, p. 162, 163] we learn that more than 100 Fourier terms are necessary to get the quality of Tables 16 and 16a.

3. Looking at the development of the parallax in the table above we see the extreme proxigean spring tide on 2011/03/19 with a (local) parallax maximum. Eight days earlier the Great 2011/03/11 Japan Quake happened. The next parallax maximum 2016/11/14 is forthcoming. From the perigee-syzygy problem in (I) we are led to the earthquake research.

3.7 Orbits and rays in Einstein's theory of relativity

Because of the curvature of space and time Kepler's First Law must be modified in relativity theory: *The orbit of a planet in the Schwarzschild space has the shape of an ellipse but there is a small revolution of the line of apsides.* The

small relativistic part of the precession of the perihelion of Mercury is a classical confirmation of Einstein's theory. An exact (ρ, φ)-formula is presented in *Über Planetenbewegung und Lichtbahnen im Schwarzschild- und im Reissner-Nordström-Raum* [8, p. 357, 358]. Surprisingly, in Reissner-Nordström space one can construct geodesic null lines with perihelion, aphelion and with a revolution of the line of apsides. So photons run through orbits customary in the moon theory – a confirmation of the duality of light; see [8, p. 369, Abb. 6].

4 Studies on the periods of the moon theory

4.1 A collection of periods

The motion of the Moon is a complicated subject with a multidude of periods. Let us compile a collection:

$U_{syn} = 29.530\,59$ days	synodic month
$U_{sid} = 27.321\,66$ days	sidereal month
$U_{ano} = 27.554\,55$ days	anomalistic month
$U_{eve} = 31.811\,94$ days	evectional month
$U_{nod} = 27.212\,22$ days	nodical or draconic month
$U_{tro} = 27.321\,58$ days	tropical month
$U_s = 365.256\,36$ days	sidereal year
$U_t = 365.242\,20$ days	tropical year
$U_a = 8.8479$ tropical years	apsides cycle, forward moving
$U_e = 1.1274$ tropical years	evectional cycle
$U_n = 18.6134$ tropical years	nodes cycle, retrograde moving
$U_p = 25800$ years	platonic year

Table 2. Months, years and cycles

The numerical values of the months and years are listed online in "Solar System Data" tables, only U_{eve} is not so common. For this reason we determined the evectional month in Section 3.5. The cycles can be calculated according to Table 3 below. Of course, the collection is not complete; for example, the old Saros period, well-known to Chinese and Babylonian astronomers, is not listed. The theory of cycles developed by Fergus Wood for the purpose of tidal dynamics in [17, II] is admirable.

4.2 Period relations

First we present a group of relations which combines months with long periods:

$\frac{1}{U_{syn}} = \frac{1}{U_{sid}} - \frac{1}{U_s}$	$U_{syn} = U_{sid} : (1 - \frac{U_{sid}}{U_s})$	$U_s = U_{sid} : (1 - \frac{U_{sid}}{U_{syn}})$
$\frac{1}{U_{ano}} = \frac{1}{U_{sid}} - \frac{1}{U_a}$	$U_{ano} = U_{sid} : (1 - \frac{U_{sid}}{U_a})$	$U_a = U_{sid} : (1 - \frac{U_{sid}}{U_{ano}})$
$\frac{1}{U_{eve}} = \frac{1}{U_{syn}} - \frac{1}{U_e}$	$U_{eve} = U_{syn} : (1 - \frac{U_{syn}}{U_e})$	$U_e = U_{syn} : (1 - \frac{U_{syn}}{U_{eve}})$
$\frac{1}{U_{nod}} = \frac{1}{U_{sid}} + \frac{1}{U_n}$	$U_{nod} = U_{sid} : (1 + \frac{U_{sid}}{U_n})$	$U_n = U_{sid} : (\frac{U_{sid}}{U_{nod}} - 1)$
$\frac{1}{U_{tro}} = \frac{1}{U_{syn}} + \frac{1}{U_t}$	$U_{tro} = U_{syn} : (1 + \frac{U_{syn}}{U_t})$	$U_t = U_{syn} : (\frac{U_{syn}}{U_{tro}} - 1)$
$\frac{1}{U_{tro}} = \frac{1}{U_{sid}} + \frac{1}{U_p}$	$U_{tro} = U_{sid} : (1 + \frac{U_{sid}}{U_p})$	$U_p = U_{sid} : (\frac{U_{sid}}{U_{tro}} - 1)$

Table 3. Period relations

These formulas will be proved in the following sections.

In order to calculate the platonic year U_p it is advantageous to use the long-period relation

$$\frac{1}{U_p} = \frac{1}{U_t} - \frac{1}{U_s}. \tag{39}$$

Proof of (39) by inserting the months in the $1/U$ formulas in rows 1, 5, 6 of Table 3. Formula (39) yields

$$\frac{U_p}{U_s} = \frac{U_t}{U_s - U_t} = \frac{365.242\,20}{365.256\,36 - 365.242\,20} = 25,794\ \textit{sidereal years}. \tag{40}$$

A 4-digit calculation with corresponding accuracy was carried out.

There is a second long-period relation:

$$\frac{1}{U_e} = \frac{1}{U_s} - \frac{1}{U_a}. \tag{41}$$

Proof of (41) by inserting the months in the $1/U$ formulas in rows 1, 2, 3 of Table 3 and by considering additionally the Harmonic Theorem (36). Formula (41) can be interpreted as the *Harmonic Theorem for Long Periods*. In Section 5.1 we will see that U_e is the long period of the beat oscillation of the lunar distance function, it is significant in earthquake statistics.

4.3 $(U_{syn} - U_{sid} - U_s)$ and the systems of coordinates

We turn to the first row "(r1)" of Table 3. U_{syn} can be calculared if U_{sid} and U_s are known. Likewise, if U_{syn} is known then U_{sid} can be determined.

For the proof of (r1) we need some steps. In Figure 3 we can see how the sidereal and synodic plane are linked; so it is natural to prove (r1) by decoding Figure 3.

First we look at the motion of Earth and Moon in the sidereal plane outside the box. The Earth circles around the Sun with constant angular velocity and in the period $\frac{1}{2}U_{sid}$ the Moon runs from M_1 to M_2. Therefore the radian measure of the angle t_2 fulfils the proportion

$$t_2 : 2\pi = \frac{1}{2}U_{sid} : U_s \tag{42}$$

with the sidereal year U_s of the Earth.

Now we look at the motion of the Moon in the synodic plane inside the box. Working with the mean value U_{syn} we assume that the Moon circles with constant angular velocity around the Earth. In the period $\frac{1}{2}(U_{syn} - U_{sid})$ the Moon runs from M_2 to M_3. Therefore the angle t_2 in the box fulfils the proportion

$$t_2 : 2\pi = \frac{1}{2}(U_{syn} - U_{sid}) : U_{syn}. \tag{43}$$

Comparing (42) and (43) we find $\frac{U_{sid}}{U_s} = 1 - \frac{U_{sid}}{U_{syn}}$ and the third equality in (r1) is proved. The other two equalities follow, q.e.d.

4.3.1 Moons of other planets

Amalthea

The relations in (r1) can also be used for forward-moving moons in the solar system with small inclination because the proof is valid in the general case. For the moon Amalthea in Jupiter's system the data

$$U^A_{sid} = 0.498^d,\ U^A_{syn} = 11^h57^m27.6^s \tag{44}$$

are given in [14, p. 127], where (d, h, m, s) are the time scales of the Earth. Obviously, $U^A_{syn} = 0.498\,236^d$; because of $0.1^s = 0.000,001^d$ only on the 6th digit an alteration ± 1 is possible. According to (r1) the period U^A_{sid} can be calculated with the same accuracy:

$$U^A_{sid} = U^A_{syn} : (1+\frac{U^A_{syn}}{U^J_s}) = 0.498\,236 : (1+\frac{0.498\,236}{4332.598}) = 0.498\,1787^d = 11^h57^m22.6^s. \tag{45}$$

So the list with the inaccurate sidereal data in [14] is not necessary. In [12] one can find our 6-digit value for the sidereal month of Amalthea.

Phoebe

For the retrograde-moving moon Phoebe in Saturn's system the data

$$U^P_{sid} = 550.337^d,\ U^P_{syn} = 523^d13^h \tag{46}$$

are given in [13]. In the retrograde case the arrangement of the months changes, $U^P_{syn} < U^P_{sid}$, and in (r1) signs have to be altered. Phoebe's plane of motion has an inclination of 150°. Looking "from below" we see an inclination of 30°. Despite this gradient we use the "plane formula" (r1), but we have to change the sign:

$$U^P_{syn} = U^P_{sid} : (1+\frac{U^P_{sid}}{U^S_s}) = 550.337 : (1+\frac{0.550.337}{10,759\,22}) = 523.5569^d = 523^d13^h22^m. \tag{47}$$

Because of $0.001^d = 1.44^m$ one can calculate the synodic period up to $\pm 2^m$ using the more accurate sidereal value and (r1).

4.4 $(U_{sid}-U_{ano}-U_a)$ and the revolution of the line of apsides

We turn to the second row (r2) of Table 3. First the inequality $U_{ano} > U_{sid}$ can be recognized, it shows the advance of the apsides.

Proof of (r2): After an anomalistic month the precession angle of the perigee is $\frac{U_{ano}-U_{sid}}{U_{sid}} \cdot 2\pi$ in radian measure because U_{sid} corresponds to 2π in the sidereal system. After $\frac{U_{sid}}{U_{ano}-U_{sid}}$ anomalistic months or $\frac{U_{sid}}{U_{ano}-U_{sid}} \cdot U_{ano} = U_a$ days the perigee of the Moon has turned around the Earth once and the third equality of (r2) is proved. The other two equalities follow, q.e.d.

4.5 $(U_{syn} - U_{eve} - U_e)$ and the evection anomaly

We turn to the third row (r3) of Table 3. Transferring the anomalistic methods we can manage the evectional problem. The anomalistic part $\frac{1}{p}\{1+e\cos(\frac{U_{syn}}{U_{ano}}\varphi)\}$ of the second level approximation (I) indicates the perigee positions with the distance $\frac{p}{1+e}$. Similarly, the evectional part $\frac{1}{p}\{1+f\cos(\frac{U_{syn}}{U_{eve}}\varphi)\}$ indicates the "evectional perigee" positions with the distance $\frac{p}{1+f}$. If both parts work together a "proxigean perigee" appears.

Proof of (r3): After an evectional month the precession angle of the "evectional perigee" is $\frac{U_{eve}-U_{syn}}{U_{syn}} \cdot 2\pi$ in radian measure because U_{syn} corresponds to 2π in the synodic system. After $\frac{U_{syn}}{U_{eve}-U_{syn}}$ evectional months or $\frac{U_{syn}}{U_{eve}-U_{syn}} \cdot U_{eve} = U_e$ days the "evectional perigee" of the Moon has turned around the Earth once and the third equality of (r3) is proved. The other two equalities follow, q.e.d.

The lunar evectional cycle U_e, the central period of this treatise, is not so common than the other cycles. For this reason we determine the numerical value:

$$U_e = \frac{U_{syn}U_{eve}}{U_{eve} - U_{syn}} = 411.785\ days = 1.1274\ tropical\ years. \qquad (48)$$

A 6-digit calculation with corresponding accuracy was carried out.

Having determined the numerical value of U_e we can remind of the second observation in [11]:

The time between the Whitsun Quake in China on 2008/05/12 and the Christmas Tsunami in Indonesia on 2004/12/26 amounts to 1233 days. On the other hand, three lunar evectional cycles take $3 \times U_e = 3 \times 411.8 = 1235$ *days.*

This observation is a hint on lunisolar structures in the earthquake distribution.

We point to three $1/U_e$ expressions:

$$\frac{1}{U_e} = \frac{1}{U_{syn}} - \frac{1}{U_{eve}} = \frac{1}{U_{ano}} - \frac{1}{U_{syn}} = \frac{1}{2}(\frac{1}{U_{ano}} - \frac{1}{U_{eve}}). \tag{49}$$

With the Harmonic Theorem (36) one can prove the equalities. The first expression is our definition in (r3) of Table 3, in the second formula we recognize the definition of Fergus Wood in [17, II, p. 2-4].

4.6 $(U_{sid} - U_{nod} - U_n)$ and the revolution of the nodes

We turn to the fourth row (r4) of Table 3. First the inequality $U_{nod} < U_{sid}$ can be recognized, it shows the retrogression of the line of nodes.

Proof of (r4): After a nodical month the retrogression angle of the nodes is $\frac{U_{sid}-U_{nod}}{U_{sid}} \cdot 2\pi$ in radian measure because U_{sid} corresponds to 2π in the sidereal system. After $\frac{U_{sid}}{U_{sid}-U_{nod}}$ nodical months or $\frac{U_{sid}}{U_{sid}-U_{nod}} \cdot U_{nod} = U_n$ days the nodes of the Moon have turned around the Earth once and the third equality of (r4) is proved. The other two equalities follow, q.e.d.

Surprisingly, the revolution period of the nodes can be determined in a good approximation by means of the sidereal periods:

$$U_{nod} = U_{sid}(1 - \frac{3}{4}(\frac{U_{sid}}{U_s})^2). \tag{50}$$

A short proof can be found in [15, II, p. 545, 546]. Combining (r4) and (50) we obtain $U_n = \frac{4}{3}\frac{U_s^2}{U_{sid}}$ days. Thus the simple approximation formula

$$\frac{U_n}{U_s} = \frac{4}{3} \cdot \frac{U_s}{U_{sid}}\ sidereal\ years \tag{51}$$

for the period of nodes is developed. Inserting the sidereal periods of the Moon we find $U_n/U_s = 17.8250$ sidereal or 17.8257 tropical years which are 96% of the observation value in Table 2.

4.6.1 The moon Deimos of Mars

The formulas (r4), (50) and (51) are valid for forward- and retrograde-moving moons in the solar system. For example, for the companion Deimos of Mars we have the result:

$$period\ of\ nodes = \frac{4}{3} \cdot \frac{779.9}{1.2624} = 823.7\ years\ of\ Mars. \tag{52}$$

In one year of Mars the retrogression angle is $26.2'$. Since the angle of inclination of the plane of motion of Deimos is $1.8°$, a station on Mars can observe the nodes and their retrogression.

4.7 $(U_{sid} - U_{tro} - U_s - U_t - U_p)$ and the gyroscope movement of the Earth

Finally we turn to the last two rows of Table 3. In [15, I, p. 22-26] Stumpff deals with the periods in the motion of Earth and Moon and proves (r5) and (r6).

In (40) we see a relation between the relatively short periods U_s and U_t on the one hand and the long platonic year U_p which is a period describing the gyroscopic moving of the Earth.

Besides the lunisolar precession of the Earth gyroscope there is also the planetary precession and the geodesic precession of the relativity theory. Because of the planetary influence the inclination of the ecliptic changes periodically. In about 40 000 years the angles sway between $21°55'$ and $24°18'$. This oscillation may be responsible for the glacial period. Are there short periods determining this long time?

4.8 Further periods and cycles

Before finishing the section with the periods we have to quote F.K. Ginzel's contribution [6] to the Encyklopädie with the title *Chronologie* which contains further periods and cycles used in old civilizations. For example, Ginzel explains the *Sirius period* of the Egyptians, the Babylonian *60 year cycles*, the *Jupiter years* of India and cycles with the names *Lustrum, Yuga, Sabbath year (every 7 years), Jubilee years, Golden years.* The classical German poet *Jean Paul* invents a chronological order for the organization of his novel *Titan* by using the stages *Jobelperiode* and *Zykel.* See Zykel 9 for further details.

5 The beat oscillation of the lunar distance function, tidal dynamics and earthquake research

With the second level approximation (I), developed in Section 3, and with the period studies in Section 4 we make it possible to uncover a beat interference.

5.1 The beat oscillation

Since the frequencies of the elliptic and evection term in (I) are only slightly different, a beat interference is generated by the first part

$$e\cos(\frac{U_{syn}}{U_{ano}}\varphi) + f\cos(\frac{U_{syn}}{U_{eve}}\varphi). \tag{53}$$

From the trigonometric formula

$$e\cos\alpha + f\cos\beta = (e+f)\cos(\frac{\alpha+\beta}{2})\cos(\frac{\alpha-\beta}{2}) - (e-f)\sin(\frac{\alpha+\beta}{2})\sin(\frac{\alpha-\beta}{2}) \tag{54}$$

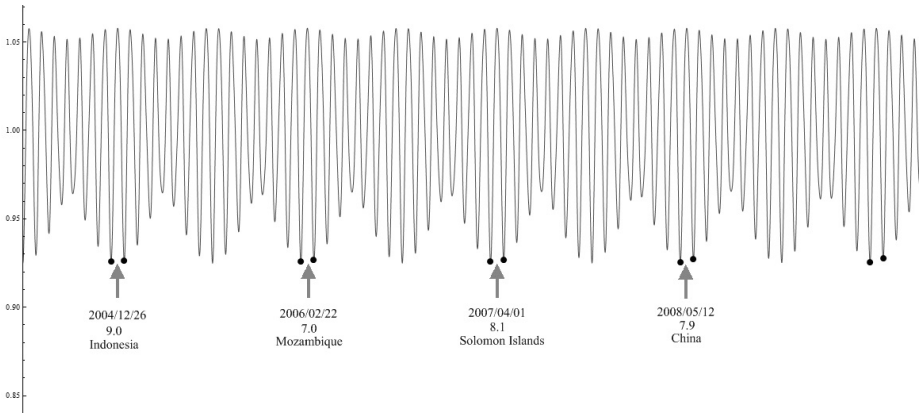

Figure 5: The beat oscillation of the lunar distance function and earthquake events

we read the long period $\frac{2}{\alpha-\beta} \cdot 2\pi$ of the interference. In our case we get

$$lpbo = \frac{2}{\frac{U_{syn}}{U_{ano}} - \frac{U_{syn}}{U_{eve}}} \cdot 2\pi[rad] = \frac{2}{\frac{U_{syn}}{U_{ano}} - \frac{U_{syn}}{U_{eve}}} \cdot U_{syn}[days] \tag{55}$$

for the long period of the beat oscillation. In the synodic plane $\varphi = 2\pi$ corresponds to U_{syn}. Fortunately we have the third expression in (49):

$$lpbo = \frac{2}{\frac{1}{U_{ano}} - \frac{1}{U_{eve}}} = U_e. \tag{56}$$

Beat Theorem: *The lunar evectional cycle U_e is the long period of the beat oscillation of the lunar distance function.*

In Figure 5 we present the r-graph of the second level approximation (I), $r = p : \{1 + \cdots\}$. We have the mean distance normalization $p = 1$ in the picture. One can see the beat oscillation, generated by the two strong terms in (53), together with a small disturbance by the variation term: the amplitude of the lower envelope of the quick oscillations is bigger than the amplitude of the upper envelope.

Trigonometric sums of type (I) – exponential sums in the language of complex analysis – are complicated mathematical objects. G.P. Meyer and the author studied exponential polynomials in Arch. Math. 36, p. 255-274, 1981.

We have to discuss a period problem. On the one hand there are the syzygys with the time period U_{syn} between the new or full moons, on the other hand the cycle

$$U_e = 411.785\ days \tag{57}$$

appeared. It can be approximated by 14 synodic months:

$$14 \times U_{syn} = 413.428\ days. \tag{58}$$

Almost every 20 years a $13 \times U_{syn}$ period must be introduced to bring syzygys and beat oscillation in a good relation.

We come back to Observation 2 in [11]:

The time between the Whitsun Quake in China on 2008/05/12 and the Christmas Tsunami in Indonesia amounts to three evectional cycles.

Figure 5 shows that both events happened in high amplitude periods of the beat oscillation.

Conjecture: *Since tide-rising force varies inversely as the third power of the lunar distance one can expect that in the high ampitude periods of the beat oscillation the seismic activity is above average.*

5.2 F.J. Wood's classification of spring tides

When the Moon is full or new, the gravitational pull of the Moon and Sun are combined and spring tides are the consequence. High spring tides occur when the Moon is close to the Earth on its elliptical path.

Wood [17, II, p. 165] presents a classification of the spring tides related to the distance of the Moon. The classes are characterized by the following intervals for parallax π:

$61'30.7'' \leq \pi < 61'32.0''$	maximun proxigean spring tides
$61'29.0'' \leq \pi < 61'30.7''$	extreme proxigean spring tides
$61'26.5'' \leq \pi < 61'29.0''$	proxigean spring tides
$60'20.0'' \leq \pi < 61'26.5''$	perigean spring tides
$59'00.0'' \leq \pi < 60'20.0''$	pseudo-proxigean spring tides
$55'00.0'' \leq \pi < 59'00.0''$	ordinary spring tides

Table 4. Classification of spring tides

Now we can impart the observation in [10]:

The first extreme proxigean spring tide in the new millennium happened on 2005/01/10 in new moon phase. Half a synodic month earlier, when the Moon was full, the 2004/12/26 Indonesia Tsunami was triggered.

This observation was a hint on lunisolar structures in the earthquake distribution. We supplement that the distance of the Moon on 2005/01/10 amounts to $\pi = 61'29.5''$ or $r = 6378.14/sin\pi = 356\,594\ km$; see [17, I, Table 16a, p. 204].

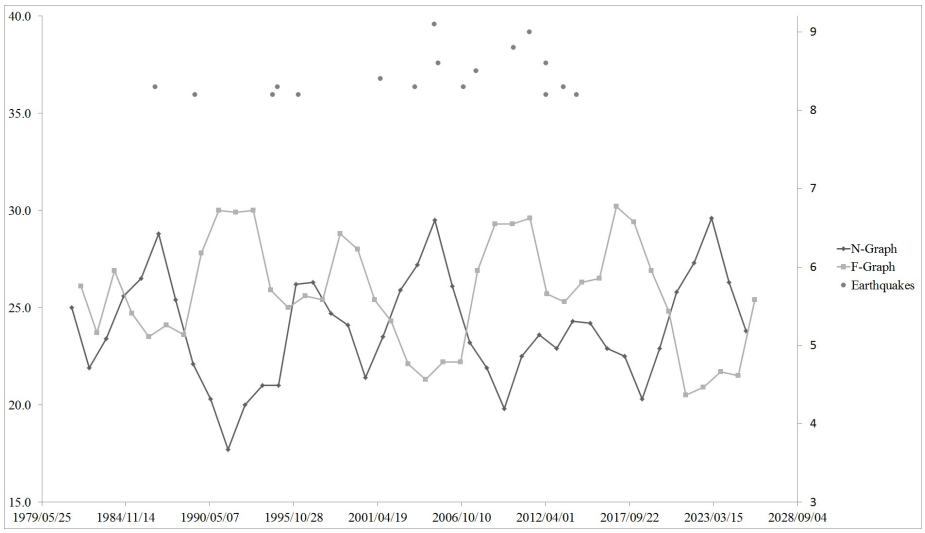

Figure 6: The N- and F-graph and the 8.2+ earthquake events

5.3 The N- and F-graph

Fergus Wood's *Tidal Dynamics* is the basis of the following investigations. In Tables 16 and 16a in [17, I, p. 159-218] lunisolar ephemerides are presented over the period 1600 – 2164. Date and parallax data we find in Cols. 2 and 4 of the Tables.

Column 2 contains the date for each case of syzygy associated with a perigee-syzygy separation $|P - S| \leq 24$ hours. The P-S hours are listed in Column 9. There appear two or three neighbouring new or full moon positions which form the boundary of synodic months. When constructing the N- and F-graph in Figure 6 we only take the dates with smallest $|P - S|$ separation and maximal parallax values into consideration.

These graphs, first introduced in [11, p. 797, Figure 1], show the global development of the distance of the Moon. For instance, one can see the peak of the N-graph:

$$2005/01/10, \quad \pi = 61'29.5'', \quad \text{extreme proxigean spring tide,}$$

and, in the upper part of the picture, the 2004/12/26 Indonesia Quake with magnitude 9.1. After *one* Saros cycle, on 2023/01/21, the next peak of the N-graph appears. Having the leap years 2008, 2012, 2016 and 2020 the Saros period amounts to 18 years and 11 days, approximately; else we have 18 years and 10 days for the cycle if there are five leap years in the interval.

Not only the peak period, but also the global development of the graphs in Figure 6 is – obviously – ruled by the Saros cycle. What is the physical reason for this phenomenon?

It is also interesting to look at the peak of the F-graph:

2011/03/19, $\pi = 61'29.6''$, extreme proxigean spring tide.

Eight days earlier the 2011/03/11 Japan Quake with magnitude 9.0 happened.

5.4 High amplitude synodic months

Using Fergus Wood's Tables 16 and 16a we constructed the N- and F-graph in Section 5.3. Now we continue these studies. Column 2 of the Tables contains the date for each case of syzygy associated with a perigee-syzygy separation $|P - S| \leq 24$ hours. The P-S hours are listed in Column 9. There appear two or three neighbouring new or full moon positions which form the boundary of synodic months. If there are two neighbouring positions, then the perigee lies in the synodic month between them, in the triple case the P-S separation of the middle point is small.

Examples: In Table 5 below one can see the N-points 2004/12/12 and 2005/01/10. Two hours before reaching the extreme proxigean N-point the Moon runs through its perigee. There are three neighbouring F-points in 2011 with $P - S = 1$ hour for the middle point.

The synodic months between the neighbouring new or full moon positions with small perigee-syzygy separation lie in the centre of the high amplitude periods of the beat oscillation of the lunar distance function. We designate these months as **high amplitude synodic months**.

How many synodic months have the high amplitude property? Let us check the problem in the new millennium. Between the new moons 2000/01/06 and 2014/01/01 we count 173 synodic months, 29 months or $29/173 = 16.8\%$ belong to the high amplitude class.

If the Moon runs through a high amplitude synodic month the lunar distance varies above average. With the distance the tension of the Earth's ellipsoidal surface varies above average. If one of the boundary points of a high amplitude synodic month is even an extreme or maximum proxigean spring tide, the variation of the tension is extreme. We bear in mind that tide-raising force varies inversely as the third power of the lunar distance.

Conjecture: *If an extreme or maximum proxigean spring tide occurs then one can reckon with an above average earthquake activity in the adjoining high amplitude synodic month or months in the triple case.*

In the period 2000/01/06 – 2014/01/01 only five synodic months of the high amplitude class begin or end with an extreme proxigean spring tide, they are listed in Table 5 below. **Thus 5/173 = 2.9% of the period are extreme critical.**

5.5 Extreme proxigean spring tides and the great earthquakes in Indonesia 2004, Chile 2010 and Japan 2011

In Table 13 in Wood [17, I, p. 141] a list of the extreme/maximum proxigean tides over the 400-year period 1600 – 1999 is compiled. We are curious to see the continuation of Wood's list in the new millennium. The first four extreme tides are presented in Table 5 together with the five adjoining high amplitude synodic months.

Date		$\pi = 61'+$	Spring tide	P-S	Mag.	Region
2004/12/12	N	8.2"	perigean	21		
2004/12/26	F				9.1	Indonesia
2005/01/10	N	29.5"	extr. proxigean	-2		
2008/12/12	F	29.3"	extr. proxigean	5		
2009/01/03					7.7	Indonesia
2009/01/11	F	15.3"	perigean	-17		
2010/01/30	F	29.3"	extr. proxigean	3		
2010/02/27					8.8	Chile
2010/02/28	F	10.5"	perigean	-20		
2011/02/18	F	3.5"	perigean	23		
2011/03/11					9.0	Japan
2011/03/19	F	29.6"	extr. proxigean	1		
2011/04/18	F	6.7"	perigean	-21		

Table 5. Strong earthquakes and extreme proxigean spring tides

Observation: *We uncover a lunisolar structure in the distribution of strong earthquakes. The 8.8+ disasters in the new millennium happened in high amplitude synodic months related to extreme proxigean spring tides. As conjectured, 2.9% of our period are extreme critical.*

In Table 5 lunisolar ephemerides and earthquake data are composed. We are glad that we can use Fergus J. Wood's grand opus on *Tidal Dynamics* together with the *Significant Earthquake Archive* of USGS.

Bearing the lunisolar structure in mind we compile, as a precaution, the next three extreme proxigean tides and their high amplitude synodic months in Table 6:

Date		$\pi = 61'+$	Spring tide	P-S
2016/10/16	F	10.1”	perigean	20
2016/11/14	F	30.2”	extr. proxigean	-2
2017/12/03	F	15.1”	perigean	17
2018/01/02	F	29.4”	extr. proxigean	-4
2022/12/23	N	3.8”	perigean	23
2023/01/21	N	29.6”	extr. proxigean	0
2023/02/20	N	4.0”	perigean	-22

Table 6. The next three extreme proxigean spring tides

The 2023/01/21 extreme tide is the ”Saros successor” of the 2005/01/10 event, with $\pi = 61'29.6''$ we find the highest parallax in new moon position in the period 1600 – 2164. The new moon N with smallest distance from the Earth in five and a half centuries is forthcoming.

The full moon F with smallest distance since 1948 will happen on 2016/11/14 with $\pi = 61'30.2''$. Its ”Saros successor” on 2034/11/25 is the next extreme tide, with $\pi = 61'30.9''$ it belongs to the maximum proxigean class in Table 4.

5.6 A physical argument for the triggering of strong earthquakes

First we look at the 9.1 Indonesia Earthquake in Table 5 with the extreme proxigean spring tide on 2005/01/10 at the end of the high amplitude synodic month. According to column 9 of Table 16a in [17, I] the perigee-syzygy separation amounts to $P - S = -2$ hours. Two hours before reaching the N-point the Moon runs through its perigee with parallax $61'29.6''$; see column 10. Because of the small $P - S$ separation the parallax at P is not much bigger than at N.

The synodic month 2004/12/12 – 2005/01/10 begins with a perigean and ends with an extreme proxigean N-point. At the full moon between the N's the lunar distance is big. In our synodic month the amplitude of the beat oscillation of the lunar distance function is extremely high.

At the perigean point the tension of the Earth's ellipsoidal surface is above average, at the extreme proxigean end point the tension is extreme. At the full moon position between the N's the lunar distance is big an the tension correspondingly small. When the Moon runs from N to F and back to N the tension varies above average. In this alteration we see the trigger of the 9.1 Indonesia Quake.

In the other three cases in Table 5 we have extreme proxigean and perigean F-points. At the new moon between the F's the lunar distance is big. When the Moon runs from F to new moon N and back to F the tension again varies above average and strong earthquakes can be expected.

For the strongest quake of the last century, the 1960 Chile Quake with magnitude 9.6 we have the data in Table 7:

Date		$\pi = 61' +$	Spring tide	P-S	Mag.	Region
1960/05/22					9.6	Chile
1960/06/09	F	18.1"	perigean	13		
1960/07/08	F	22.4"	perigean	-9		

Table 7. Chile 1960

The 9.6 Chile Quake occured 18 days before the high amplitude synodic month 1960/06/09 – 1960/07/08. We think of the third experiment of Christoph Gackstatter in [11, p. 801]: *An above average number of strong 7.5+ earthquakes happen in times when the oscillation amplitude of the lunar distance function is increasing.* Tense tectonic plates can be loosened by oscillations of the tide-raising forces.

Fourteen 8.5+ earthquakes happened since 1950. Four of them fall into high amplitude months, four into the adjoining months which also belong to the high amplitude periods.

Even the Great Lisbon Earthquake, triggered on the All Saint's Day of 1755, is an example for our physical argument.

Date		$\pi = 61' +$	Spring tide	P-S	
1755/11/01					Great Lisbon Quake
1755/11/04	N	26.2"	perigean	6	
1755/12/03	N	15.4"	perigean	-16	

Table 8. The Great Lisbon Quake

The Lisbon Earthquake occured three days before the high amplitude synodic month specified in Table 8. Voltaire, Kant, and Goethe report on this disaster. Being acquainted with this literature Heinrich von Kleist created the dramatic story *Das Erdbeben von Chili* where the 1647/05/13 Chile quake is in the background. According to Wood's Table 16 the date lies in a low amplitude period of the beat oscillation.

Statement: *One cannot predict earthquakes. Multi-layered effects work together when earthquakes are created. If a strong earthquake happens in a high amplitude period of the distance function of the Moon, the lunisolar forces have made a contribution to the triggering of the quake.*

6 Timing and location of quakes

In an internet publication (PhysOrg.com 2009) we find the report "Quake Prediction Model Developed" with the statement: "The forecasting model developed by Danijel Schorlemmer aims to predict the rough size and location of future quakes. While the timing of quakes remains unpredictable, progress on two out of three key questions is significant in the hard discipline of earthquake forecasting."

In the present treatise we deal with the third key question. By using Fergus Wood's tables in [17, I] we determined the extreme and maximum proxigean spring tides and the adjoining high amplitude synodic months. These months are critical time periods and strong earthquakes can be expected. Now we are faced with the problem to find connecting lines between timing and location research.

6.1 The prehistory of the 9.1 Indonesia Quake

We have to select suitable intervals for a rectangular earthquake search in the *Significant Earthquake Archive* of USGS [18]. In a first experiment we take the geographical neighbourhood

$$15^\circ N \; to \; 15^\circ S, \; 85^\circ E \; to \; 115^\circ E \tag{59}$$

of the point $(3.295^\circ N, 95.982^\circ E)$ south of Sumatra where the 9.1 Quake happened. The Andaman Islands, Sumatra and Java belong to rectangular (59). The maps in the *Earthquake Archive* show the distribution of the quakes along the Java Trench. When looking at the 6.0+, 6.5+, ... earthquakes in the rectangular $15^\circ N \; to \; 15^\circ S, \; 85^\circ E \; to \; 130^\circ E$ in the time after 1986/12/31 we find a gap in the distribution: the $115^\circ E$ meridian divides the Java and Timor Trench earthquakes. We only consider quake events in the west of the gap and choose $115^\circ E$ as the right border line in (59).

Let us start our investigation with the 1986/12/31 peak of the N-graph in Figure 6 in Section 5.3. This way we have the whole Saros cycle before the 2004 Indonesia disaster in our program.

Interested in strong earthquakes we find out that only three 7.5+ events happened before the Great 2004 Indonesia Quake. These 7.5+ predecessors fall into high amplitude periods of the beat oscillation of the lunar distance function. The lunisolar forces have made a contribution to the triggering of the quakes. After 2004/12/26 the density of the 7.5+ earthquakes increased. Interested in the seismic activity in the high amplitude synodic months and in the neighbouring synodic periods we count the 4.5+, 6.0+ and 7.5+ quakes happening in these months in Table 9.

Synodic months		4.5+	6.0+	7.5+
1994/03/27 – 1994/04/25	h.a.s.m.	7	0	0
1994/04/25 – 1994/05/25		38	3	0
1994/05/25 – 1994/06/23		169	6	1
1994/06/23 – 1994/07/22		21	0	0
2000/05/04 – 2000/06/02		14	0	0
2000/06/02 – 2000/07/01		209	5	2
2000/07/01 – 2000/07/31	h.a.s.m.	34	0	0
2004/11/12 – 2004/12/12		13	0	0
2004/12/12 – 2005/01/10	h.a.s.m.	689	21	1
2005/01/10 – 2005/02/08		727	2	0
2005/02/08 – 2005/03/10		156	2	0

Table 9. Synodic months and the number of earthquakes in rectangular (59)

The high amplitude synodic months are marked with h.a.s.m. The *Significant Earthquake Archive* of USGS [18] yields the numbers in Table 9. There are no overlaps because we insert time intervals of type 1994/03/27 00:00:00 – 1994/04/25 00:00:00 in the first column of Table 9.

6.2 The prehistory of the 9.0 Japan Quake

We have to select suitable intervals for a rectangular earthquake search in the *Significant Earthquake Archive* of USGS [18]. In a first experiment we take the geographical neighbourhood

$$45^\circ N \; to \; 35^\circ N, \; 135^\circ E \; to \; 146^\circ E \tag{60}$$

of the point ($38.297^\circ N$, $142.373^\circ E$) near the east coast of Honshu where the 9.0 Quake happened. The quakes along the Kuril Islands are omitted.

Let us start our investigation with the 1993/03/08 peak of the F-graph in Figure 6 in Section 5.3. This way we have the whole Saros cycle before the 2011 Japan disaster in our program.

Interested in strong earthquakes we find out that only three 7.5+ events happened before the Great 2011 Japan Quake. Two of these 7.5+ predecessors fall into high amplitude periods of the beat oscillation of the lunar distance function. The lunisolar forces have made a contribution to the triggering of the quakes. After 2011/03/11 the density of the 7.5+ earthquakes increased. Interested in the seismic activity in the high amplitude synodic months and in the neighbouring synodic periods we count the 4.5+, 6.0+ and 7.5+ quakes happening in these months in Table 10.

Synodic months		4.5+	6.0+	7.5+
1993/07/03 – 1993/08/02		78	3	1
1994/11/03 – 1994/12/03	h.a.s.m.	8	0	0
1994/12/03 – 1995/01/01		52	6	1
1995/01/01 – 1995/01/30		50	2	0
1995/01/30 – 1995/03/01		16	2	0
2003/08/27 – 2003/09/26		25	2	1
2003/09/26 – 2003/10/25		109	3	0
2003/10/25 – 2003/11/23	h.a.s.m.	44	1	0
2003/11/23 – 2003/12/23	h.a.s.m.	15	0	0
2011/01/19 – 2011/02/18		12	0	0
2011/02/18 – 2011/03/19	h.a.s.m.	1500	55	3
2011/03/19 – 2011/04/18	h.a.s.m.	743	11	0
2011/04/18 – 2011/05/17		238	3	0

Table 10. Synodic months and the number of earthquakes in rectangular (60)

6.3 Common properties

In Tables 5 and 6 in Section 5.5 we presented nine high amplitude synodic months which begin or end with an extreme proxigean spring tide. The great earthquakes in Table 5 show that these months are extreme critical. Faced with the problem to find critical geographical regions we studied the seismic prehistory of the Great Indonesia and Japan Quake.

In the geographical neighbourhood (59) of the point where the 9.1 Indonesia Quake happened and in the Saros cycle before the event we discovered a low earthquake activity with two short-term runaways caused by above average lunisolar forces. Then, in the extreme critical synodic month 2004/12/12 – 2005/01/10 the Great Indonesia Quake happened. A backlog demand for strong earthquakes can be recognized. A similar observation we made in the neighbourhood (60) of the point where the 9.0 Japan Quake occured.

It would be desirable to compile a list of geographical regions with the above mentioned properties: low earthquake activity with short-term runaways in high amplitude periods of the lunar distance function. In these short-term runaways we see *one* indicator for the development of a strong earthquake if an extreme or maximum proxigean spring tide lies ahead.

7 Earthquake statistics with Student's t-test

Influences the Moon the creation of earthquakes? This question was discussed controversial in the past. Now we have a statistically significant result on the problem.

In 2010 Christoph Gackstatter made a complete statistical test for the entirety for measured quakes. More than 650,000 earthquakes and 13,860 observations, which is the total number of days in the database, are used for the linear regression; see [11, p. 800-804]. With the small 1.83% p-value a fundamental result is proved:

The lunar evection anomaly, discovered by Hipparcos and installed in Ptolemy's epicycle theory, has a statistically significant influence on the earthquake distribution.

In our computer epoch statistics can handle huge observation data.

We present the steps of Christoph Gackstatter's proof.

7.1 The beat envelopes

In the preceding sections our study was mainly focused on large single earthquake events, now we turn to the entirety of measured quakes.

Conjecture: *According to the previous research it is highly probable that the beat oscillation of the lunar distance function with the evectional period* $U_e = 411.8$ *days has an influence on the distribution of earthquakes.*

To test the conjecture we introduce the auxiliary function

$$f(t) = -\cos(\frac{2\pi}{205.892\,days}t) \tag{61}$$

with the period $U_e/2$ of the beat envelopes; see the lower graph in Figure 7. Hence, if the amplitude of the fast oscillations is maximal the above function is -1 and if the amplitude of the fast oscillations is minimal the above function is $+1$.

The data of our statistical test cover the time from 1973/01/01 to 2010/12/12. So it is advantageous to fix the initial point $f(0)$ at an extreme proxigean full moon position in the centre of the time period. The best choice we find in Wood's Table 16:

1993/03/08 F 61'30.0" extreme proxigean P-S = -2 .

From this point the f-values of all the other days can easily be calculated. For instance, for the extreme proxigean full moon on 1976/02/26 we find $f(t) = -0.9942$. The minima of $f(t)$ are close to the dates of the points of the N- and F-graph.

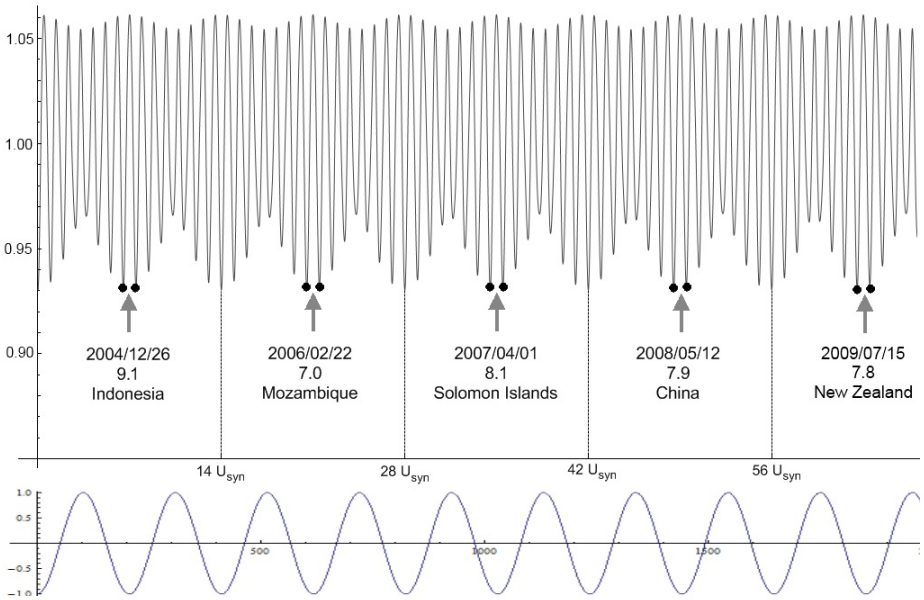

Figure 7: The beat oscillation of the lunar distance function, earthquake events and the auxiliary function $f(t)$

7.2 Earthquake data

Earthquake data are provided by the website of the National Earthquake Information Center. Four particular data sets are created:

- total number of earthquakes per day,
- number of earthquakes with magnitude ≥ 6 per day,
- number of earthquakes with magnitude ≥ 7.5 per day,
- $\sum_{i \in day} 10^{magn(i)}$ per day.

The last data set is created in order to give higher weights to stronger earthquakes. Figures B1, B2, B3 and B4 in [11] show plots of the sets over the given time period.

7.3 Methodology and results

Christoph Gackstatter used Student's t-test and 90% confidence intervals to check whether or not there is a relationship between the evectional beat cycle and earthquake statistics.

1^{st} **experiment.** In a first experiment he tested whether $f(t)$ and the earthquake statistics are directly related by considering daily observation. More than 650,000 earthquakes and 13,860 observations are used for the linear regression.

The most striking detail of the first experiment is the smallness of the p-value for the total count. With p-value = 1.83% a significant relationship between the total number of earthquakes per day and the evectional beat interference is uncovered. The evection anomaly has a significant influence on the earthquake distribution.

2^{nd} **experiment.** Secondly, Christoph Gackstatter tested whether there are more (or stronger in the case of the fourth data set) earthquakes when $f(t)$ is negative. One can do this by summing up the earthquake count for $f(t) < 0$ and connect it with the dummy variable 1. The same is done for $f(t) > 0$ and the dummy variable 0. Here only 134 observations can be used since one observation has the length $U_e/4 = 102.964\,days$. No significant result is found.

3^{rd} **experiment.** In a third experiment the slope of $f(t)$ is in the centre of interest. One can assume that there are more earthquakes when the slope is negative (oscillation amplitude is increasing) and vice versa, again using dummy variables and 134 observations.

The most interesting result of the experiment is the smallness of the p-value for the third data set. With the p-value = 7.96% an above average number of strong 7.5+ earthquakes happen in times when the oscillation amplitude of the lunar distance function is increasing. In general, the slope of $f(t)$ is negative in the $3\frac{1}{2}$ months period before the dates of the points of the N- and F-graph. In Figure 7 four 7.8+ examples are listed which happen in the synodic month before points of the N-graph.

8 Epilogue

8.1 New insights into old astronomical cycles

The structure of the Saros eclipse cycle

The Saros period, well-known to old civilizations, specifies the time difference between eclipse phenomena. It is because 223 synodic, 239 anomalistic and 242 draconic months are nearly commensurate.

In [11] we gained a new insight into the cycle. Figures 6 and 7 complement one another. In Figure 6 we count 16 intervals on the N-graph between the peaks and there are 14 synodic months between the high parallax N-points in Figure 7, in general. Approximately every 18 years, for example in 1993/94 and 2012/13, a $13 \times U_{syn}$ period occurs for compensation reasons. So we find $16 \times 14 - 1 = 223$ synodic months or *one* Saros period between the peaks of the N-graph. A factorization of the Saros cycle is uncovered.

The lunar evectional cycle U_e

The grand observer Hipparcos discovered the lunar evection anomaly. Ptolemy pays attention to the anomaly when creating his epicycle theory.

Fergus J. Wood pointed to the importance of the evectional cycle U_e in tidal dynamics; see [17, II, p. 2-4]. In formula (49) in Section 4.5 we present defining expressions for U_e.

Since the frequencies of elliptic inequality and evection anomaly in the motion of the Moon are only slightly different a beat interference occurs. In Section 5.1 we proved the Beat Theorem: *U_e is the long period of the beat oscillation of the lunar distance function.* Since tide-raising force varies inversely as the third power of the distance of the Moon, one can expect that in the high amplitude periods of the beat oscillation the seismic activity is above average.

This conjecture is proved true. In 2010 Christoph Gackstatter made a complete statistical test and showed: *The lunar evection anomaly has a statistically significant influence on the earthquake distribution.* See [11, p. 800-804] and section 7 for further details.

8.2 Interdisciplinarity

Seismology, one of the main sections of geophysics, is the study of earthquakes and the movement of vibrations through the interior of the Earth. Earthquake forecasting and lab simulations of geological processes are topics of seismic research.

In recent times biological methods are developed to predict earthquakes and other disasters. We mention the *Disaster Alert Mediation using Nature (DAMN)* program of M. Wikelski. Animal behaviour can be incorporated into earthquake forecasting. For example, toads left the breeding colony days before the 2009/04/06 L'Aquila Quake in central Italy.

In the present treatise the lunisolar effect on the trigger of earthquakes was studied, critical time periods are listed in Section 5.5. Strong earthquakes happened in synodic months which begin or end with an extreme proxigean spring tide. So a question on the $DAMN$ research arises: can one discover a strange behaviour of animals in these critical periods. The synodic month 2016/10/16 – 2016/11/14 is the next dangerous time with an extreme proxigean spring tide at the end of the month.

Finally we remember of David Hilbert's Thesis: *We must know, we will know.* In the hard discipline of earthquake forecasting we must bring together geophysics, biology, and astronomy to improve the prediction possibilities. The determination of critical regions would be a success. We have a problem with the determinism in the second part of Hilbert's Thesis.

8.3 Appendix: The 2015/09/16 Chile Quake with magnitude 8.3

The strong earthquake in Chile integrates into our system:

Date		$\pi = 61'+$	Spring tide	P-S	Mag.	Region
2015/08/29	F	4.8"		21		
2015/09/16					8.3	Chile
2015/09/28	F	26.5"	proxigean	-1		
2015/10/27	F	1.3"		-23		

Table 5a. Chile 2015

The Chile Quake happened in the high amplitude synodic month before the 2015/09/28 proxigean spring tide.

9 References

Classical Literature (arranged in a chronological order)

[1] Johannes Kepler: *Astronomia Nova* (Prag 1609) and *Harmonices Mundi Libri V* (Linz 1619). Besides Kepler's original title the abbreviation *Harmonice Mundi* without the "s" of the genitive is used. We will cite [1, AN] and [1, HM]. Kepler finished his book on the harmonies in the world on May 27, 1618, four days after the Defenestration of Prague, marking the outbreak of the 30 Years War. There is a German translation of the two books by M. Caspar. An English translation of the *Astronomia Nova* has been done by W.H. Donahue, a translation of the *Harmonice Mundi* by E.J. Aiton, A.M. Duncan and J.V. Field.

[2] R. Westfall: *Isaak Newton. Eine Biographie.* Spektrum Akad. Verlag, Heidelberg, Berlin, Oxford 1996. The English original with the title *The Life of Isaak Newton* was published at Cambridge Univ. Press in 1993.

[3] A. Koestler: *Die Nachtwandler. Die Entstehungsgeschichte unserer Welterkenntnis.* Suhrkamp, München 1980. The English original with the title *The Sleepwalkers* was published in 1959.

[4] Leonhard Euler: *Theoria motus lunae* (Berlin 1753) and *Theoria motuum lunae* (Petropoli 1772). Besides these two lunar theories there are further important contributions to celestial mechanics and astronomy in Euler's grand opus; see [9] for further details.

[5] G.W. Hill: *Researches in the lunar theory.* Amer. Journ. Math, 1, 5-26, 129-147, 245-260, 1877. *On the part of the motion of the lunar perigee which is a function of the mean motions of the Sun and Moon.* Cambridge USA, 1877 and Acta Math. 8, 1-36, 1886.

[6] F.K. Ginzel: *Chronologie.* Enc. Math. Wiss., Band VI, 366-376, 1910.

[7] E.W. Brown: *Theorie des Erdmondes.* Enc. Math. Wiss., Band VI, 667-728, 1914.

Further References (arranged in an alphabetical order)

[8] F. Gackstatter: *Über Planetenbewegung und Lichtbahnen im Schwarzschild- und im Reissner-Nordström-Raum.* Ann. Phys. (Leipzig) 40, 352-374, 1983.
[9] F. Gackstatter: *Eulers Beiträge zu Variationsrechnung und Himmelsmechanik.* Sitzungsber. Leibniz-Soz. Berlin, Band 94, 57-65, 2008.
[10] F. Gackstatter: *Lunisolar effect on spring tides, earthquakes, and tsunamies.* Journal of Coastal Research 23, 528-530, 2007.
[11] F. Gackstatter, C. Gackstatter: *Lunisolar effect on the trigger of earthquakes.* Astron. Nachr. 332, 795-804, 2011.
[12] S. v. Hoerner, K. Schaifers: *Meyers Handbuch über das Weltall*, 2. Edition. Bibliogr. Institut, Mannheim 1961.
[13] P. Moore, I. Nicolson, P. Cattermole: *Atlas des Sonnensystems.* Herder, Freiburg 1985.
[14] P. Moore: *Der grosse Atlas des Universums.* Orbis, München 1993.
[15] K. Stumpff: *Himmelsmechanik*, 3 Volumes. VEB Deutscher Verlag Wiss. Berlin 1959, 1965 and 1974.
[16] V. Szebehely: *Theory of Orbits. The Restricted Problem of Three Bodies.* Academic Press, New York 1967.
[17] F.J. Wood: *Tidal Dynamics*, 2 Volumes. Journal of Coastal Research, Special Issues 30 and 31, 2001.
[18] USGS: *Significant Earthquake Archive*, 2014.
[19] F. Gackstatter: *Lunisolarer Einfluss auf die Entstehung von Erdbeben.* Leibniz Online 19/2015.